

Article

Metal Composition and Source Identification of PM_{2.5} and PM₁₀ at a Suburban Site in Pathum Thani, Thailand

Sasikarn Nuchdang¹, Wilasinee Kingkam¹, Udomrat Tippawan², Wiranee Sriwiang¹, Ratchai Fungklin³ and Dussadee Rattanaphra^{1,*}

¹ Nuclear Technology Research and Development Center, Thailand Institute of Nuclear Technology (Public Organization), Nakhon Nayok 26120, Thailand

² Department of Physics and Materials Science, Faculty of Science, Chiang Mai University, Chiang Mai 50200, Thailand

³ Nuclear Technology Service Center, Thailand Institute of Nuclear Technology (Public Organization), Nakhon Nayok 26120, Thailand

* Correspondence: dussadeer@tint.or.th

Abstract: This study reports the mass concentrations, elemental characterization and identification of the possible sources of PM_{2.5} and PM₁₀ at a suburban site in Pathum Thani, Thailand. The sampling was done from 18 February 2021 to 14 September 2021. PM_{2.5} concentrations were between 0.39 µg/m³ and 174.26 µg/m³, while PM₁₀ concentration ranged from 12.75 µg/m³ to 242.02 µg/m³. The average concentration of PM_{2.5} in the wet season (61.96 µg/m³) in the study area exceeded the national ambient air quality standards (NAAQS). Particle-induced X-ray emission (PIXE) was used to measure the element concentrations. The main elements, namely Fe, K, Cr and Ca, in both PM_{2.5} and PM₁₀ showed significantly higher concentrations in the summer season. A qualitative inter-elemental correlation analysis, principal component analysis (PCA) and cluster analysis (CA) were applied for source identification of PM_{2.5} and PM₁₀. The results for the three procedures were in good agreement. Four and three factors of sources were isolated by the PCA for PM_{2.5} and PM₁₀, respectively. The main sources identified by PCA were, for PM_{2.5}, soil dust and biomass burning (32%), road dust and industrial emission (25%), vehicle and industrial emission (10%) and soil dust (9%); for PM₁₀, road dust and industrial emission (36%), crustal and biomass burning (30%) and industrial sources (10%).

Keywords: PM_{2.5}; PM₁₀; principal component analysis; cluster analysis; correlation analysis



Citation: Nuchdang, S.; Kingkam, W.; Tippawan, U.; Sriwiang, W.; Fungklin, R.; Rattanaphra, D. Metal Composition and Source Identification of PM_{2.5} and PM₁₀ at a Suburban Site in Pathum Thani, Thailand. *Atmosphere* **2023**, *14*, 659. <https://doi.org/10.3390/atmos14040659>

Academic Editor: Pilar Fernández Ramón

Received: 13 February 2023

Revised: 13 March 2023

Accepted: 23 March 2023

Published: 31 March 2023



Copyright: © 2023 by the authors. Licensee MDPI, Basel, Switzerland. This article is an open access article distributed under the terms and conditions of the Creative Commons Attribution (CC BY) license (<https://creativecommons.org/licenses/by/4.0/>).

1. Introduction

Thailand is facing problems with air quality issues, resulting in adverse health consequences. It also has serious effects on climate forcing [1,2], global warming [2,3] and visibility [1,4]. The most polluted substances include particulate matter (PM_{2.5} and PM₁₀) and gaseous species (sulfur dioxide; SO₂, nitrogen dioxides; NO₂, carbon monoxide; CO, hydrocarbon, etc.). Among air pollutants, air particulate matter (APM), PM_{2.5} (fine particles with a diameter <2.5 µm), and PM₁₀ (coarse particles with a diameter between 2.5 and 10 µm) draw considerable attention because of their high contribution to air pollution and the detrimental health effects such as respiratory and cardiovascular disease [5,6], visibility effects [4,7] and climate change [1,2]. The levels of PM_{2.5} and PM₁₀ are monitored by Thailand's Pollution Control Department (PCD). It revealed that every year, a high concentration of PM_{2.5} is found from January to April and peaks around March, while the concentration of PM₁₀ reaches from December to February and peaks around January. In 2019, the concentration of PM_{2.5} in Bangkok ranged from 4–104 µg/m³ and exceeded the national ambient air quality standards (NAAQS) for 34 days, while the concentration of PM_{2.5} in Chiang Rai, the northern area of Thailand, reached 353 µg/m³ which is seven times higher than the standard level. In addition, a high concentration of PM_{2.5} and PM₁₀

can be found in central parts of Thailand, including Pathum Thani, Samut Prakan, Samut Sakhon, Nonthaburi and Saraburi.

The main sources of PM_{2.5} and PM₁₀ in Thailand are automobiles, agriculture activities (crop residue burning; rice, cassava, sugarcane, soybean, potato, etc.; wildfires, and others related to agriculture industries) [8–13] and the industrial sector (petroleum refinery, natural gas separation, iron and steel, cement, production of rubber, thermal power plant, etc.) [9,12–14]. There have been a number of reports mentioning the possible sources of PM_{2.5} and PM₁₀ in Thailand. Ahmad et al. (2022) [13] reported that the major sources of PM_{2.5} and PM₁₀ in three areas of Bangkok (Ari, Din Daeng and Bangna) were local emission sources and sea salt, while vehicle emissions, coal combustion, biomass burning, secondary aerosol formation, industrial emissions and dust were found to be the most significant local sources of PM_{2.5} and PM₁₀. Moreover, the health risk assessment of heavy metals revealed that the Cr in PM_{2.5} and PM₁₀ had a carcinogenic risk to adults in Bangna and Din Daeng. The carcinogenic risk value of Cr exceeded the permissible limits, which is the most serious threat to the residents of Bangkok. Vongruang and Pimonsree (2020) [15] applied the WRF-CMAQ modeling system for source identification of PM₁₀ in mainland Southeast Asia (MSEA), including Laos, Myanmar, Cambodia, Thailand, China, and Vietnam. It was found that the main source of PM₁₀ was biomass burning which contributed 49% in MSEA, while it specifically contributed 45% in Thailand. Choochuay et al. (2020) [12] mentioned that the level of PM_{2.5} in Bangkok was affected by both local (vehicular exhausts) and regional (biomass-burning) sources. Hierarchical cluster analysis (HCA) results also revealed that the major sources of PM_{2.5} were a mixture of combustion activities (biomass burning, vehicular exhausts, fossil fuel, coal and industrial emissions). In addition, PCA extracted five important sources of PM_{2.5}, including vehicular exhausts, biomass burning, sea salt aerosols, power plants, and industrial emissions. Kanjanasiranont et al. (2022) [8] investigated the concentrations and chemical compositions of PM₁₀ in Bangkok and its vicinity areas, including Nonthaburi and Nakhon Pathom, Thailand. C, O and Si were found to be primary components with minor and trace elements, including Fe, Cu, Cr, Ca, Na and S. These elements indicated that their origin might be related to road dust, vehicle emission, and the erosion of building products. Kayee et al. (2020) [11] studied the metal concentrations and source apportionment of PM_{2.5} in Chiang Rai, the northern part of Thailand and Bangkok from January–April 2019. The results showed that the possible sources extracted by PCA for Chiang Rai were (1) crustal dust and biomass burning, (2) industrial sources, and (3) refuse incineration mixed with road dust; for Bangkok, (1) natural background, industrial emissions and coal combustion, (2) traffic emission, and (3) sea spray. In addition, high concentrations of crustal metals and an increase in the Pb isotope ratio (²⁰⁶Pb/²⁰⁷Pb) in Chiang Rai were noted during the haze. Kawichai et al. (2022) [16] studied the source identification of PM_{2.5} during a haze period (January–May 2017) in Chiang Mai, the northern area of Thailand, using stable carbon ($\delta^{13}\text{C}$) and nitrogen isotopes ($\delta^{15}\text{N}$). The results indicated that biomass burning was the main source of PM_{2.5}, to which C₃ and C₄ plants contributed about 74% and 26%, respectively.

As shown in the aforementioned reports, most research focuses on the studies of source identification of PM_{2.5} and PM₁₀ in urban sites, Bangkok and the northern part of Thailand, Chiang Mai and Chiang Rai, while only a few studies have been conducted on source identification of both PMs in the suburban area of Thailand, especially Pathum Thani. Pathum Thani is one of the central provinces located right next to Bangkok. It has many important industrial estates which produce steel wires, electronic parts, food processing, metal processing, etc. Pathum Thani also has many universities and academic and research institutes. Moreover, there are a large number of rice paddies and other crop-growing areas. There have been reports that Pathum Thani is facing an air pollution crisis [17]. The PCD recorded that the levels of PM_{2.5} in the Khlong Luang district, in Pathum Thani, reached 88, 74, and 79 $\mu\text{g}/\text{m}^3$ in 2019, 2020, and 2021, respectively, which exceeded the state standard. A previous study has shown that the main contributing sources to PM_{2.5} in the Klongha

district in Pathum Thani were traffic and biomass burning, while soil and construction were the major sources of PM_{10} [18].

This work measured the mass concentrations of $PM_{2.5}$ and PM_{10} in summer and wet seasons from 18 February 2021 to 14 September 2021 at a suburban site in Pathum Thani, Thailand. The seasonal variations of mental concentration were determined by the particle-induced X-ray emission (PIXE) technique. In addition, the sources of both $PM_{2.5}$ and PM_{10} were identified by inter-element correlation, cluster analysis (CA) and principal component analysis (PCA).

2. Materials and Methods

2.1. Study Area Description

Thailand is a tropical country located at 6° – 20° latitude north and 98° – 105° longitude East. As Thailand is situated so close to the equator, it experiences hot and humid temperatures all year round. The average temperature in Thailand ranges from 18 to $38^{\circ}C$, and the mean annual rainfall varies from 1000–1800 mm.

Pathum Thani is part of the Bangkok Metropolitan Region (BMR) and is situated approximately 40 km north of Bangkok. It covers an area of 589 sq. km and has a population of 938,000. Most areas of the city are plains, with two rivers. The Chao Phraya River flows through the heart of the district, Muang district. The sampling site ($14.24^{\circ}N$, $100.43^{\circ}E$) was located at a height of about 2 m above ground level in the Thailand Institute of Nuclear Technology, Khlong Luang district, Pathum Thani Province, Thailand (Figure 1). The site is influenced by a complex mixture of residential, commercial, agricultural and industrial emissions. It is surrounded by houses (wooden and brick), a canal, a paddy field and a field crop. The monitoring site also hosts many large and medium-scale industries such as semiconductors, steel wires, electronic power equipment, motor, machine tools and metal processing. These industries are located approximately 20 km northwest of the monitoring site.

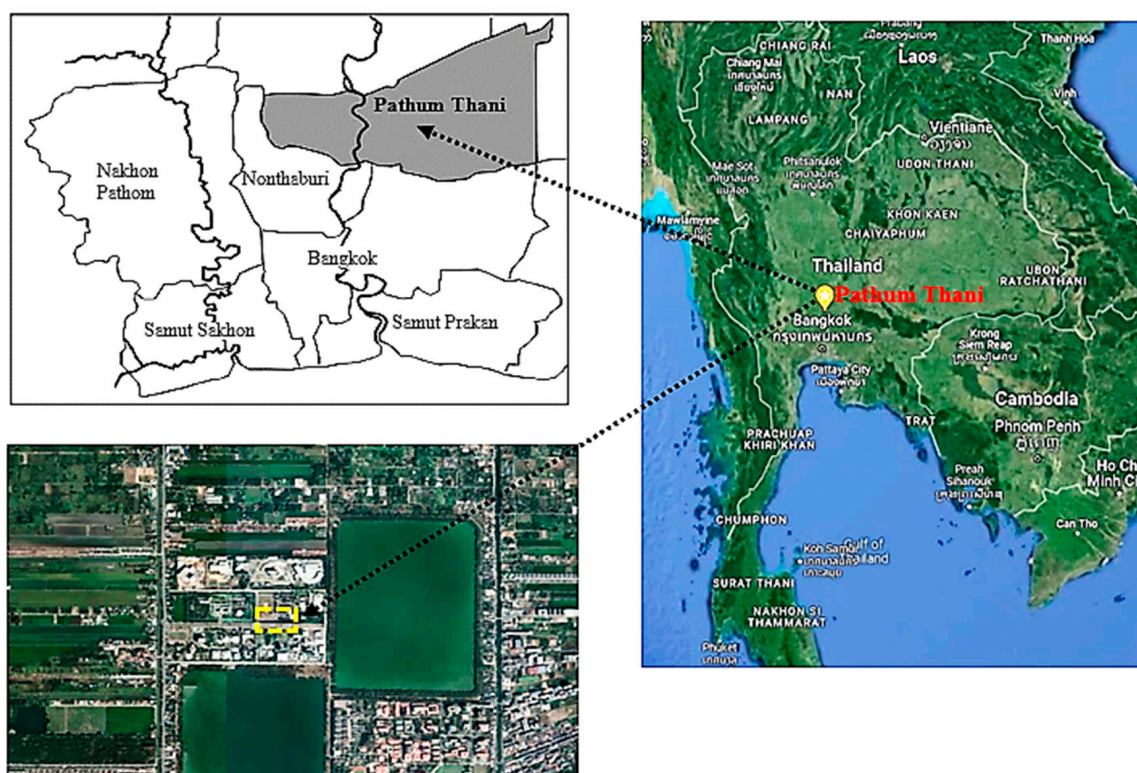


Figure 1. Location of sampling site.

2.2. Sampling Procedure and Instrumentation

PM_{2.5} and PM₁₀ sampling were carried out using a Tisch TE-Wilbur sampler (Low volume air sampler) according to the Federal Reference Method (40 CFR, Part 53, 50 Appendix L). Samples were collected on 46.2 mm PTFE filters for 2–3 days a week for PM_{2.5} and PM₁₀, respectively, at a flow rate of 16.67 L/min for 24 h. Sampling started at 9 a.m. and ended at 9 a.m. the next day. PM_{2.5} and PM₁₀ sampling were done continuously from the 18 February 2021 to the 14 September 2021. Each filter was stored in a polyethylene bag and conditioned in an auto-desiccator at 25 °C and 40–50% relative humidity at least 24 h before and after sampling; then, they were weighed on a digital microbalance (Mettler-Toledo; sensitivity of 0.001 mg) to determine the gravimetric mass of PM_{2.5} and PM₁₀. Due to the filter samples used in this study being PTFE, they are non-hygroscopic and possess low sensitivity to variations of temperature and humidity due to their permanent hydrophobicity, hence they have the great ability to limit water absorption [19]. In total, 77 samples of PM_{2.5} (31 during summer and 46 during the wet period) and 49 samples of PM₁₀ (21 during summer and 28 during the wet period) were collected. The sampling parameters are summarized in Table 1.

Table 1. Sampling parameters.

Parameters	Data
Sampling site	14.24° S, 100.43° E
Sampling period	18 February 2021–14 September 2021 Summer season (18 February 2021–15 May 2021) Wet season (16 May 2021–14 September 2021)
Total number of samples collected	
PM _{2.5}	77 (31 for summer; 46 for wet period)
PM ₁₀	49 (21 for summer; 28 for wet period)
Average sampling time (h)	24
Average flow rate (L min ⁻¹)	16.67
Average volume (m ⁻³)	24

Meteorological parameters, including temperature, relative humidity, atmospheric pressure, wind speed and rainfall, were collected from Khlong Nueng station, Pathum Thani, located approximately 18 km from the motoring site, as provided by the National Hydroinformatics Data Center available online (www.tiwrn.hii.or.th/v3/ (accessed on 15 September 2021)).

2.3. Elemental Analysis

The collected PM_{2.5} and PM₁₀ samples were analyzed by the PIXE technique for the measurement of elemental composition. The PIXE measurements were performed using 2 MeV proton by 1.7-MV Tandetron tandem accelerator at the Department of Physics and Materials Science, Faculty of Science, Chiang Mai University, Thailand. The X-rays emitted were detected by means of a Si (Li) detector (Mirion Technologies (Canberra), Inc., Meriden, CT, USA). PIXE spectra were determined using the GUPIX software. The energy resolution of the detection system was determined by using a standard 304 stainless steel sample. The resolution was estimated from the full width at half maximum (FWHM) of the Fe K α 1 peak at 6.4 keV to be 180 eV \pm 10 eV. Calibration of the PIXE system was performed by irradiating the suitable Micro Matter thin target standards [20]. The precision and accuracy of the PIXE technique are typically within \pm 15%. Detailed parameters are shown in Table 2.

Table 2. Parameters for PIXE analysis used in this study.

Analysis Equipment	Tandemron Tandem Accelerator at Department of Physics and Materials Science, Faculty of Science, Chiang Mai University, Thailand
Proton energy	2 MeV
Detector	Si(Li)
Beam intensity	2 nA
Beam spot area	1 mm ²
Analysis time	1000 s
Analysis software	GUPIX

2.4. Source Identification Methods

Three multivariate methods, principal component analysis (PCA), cluster analysis (CA) and Pearson correlation analysis, were used to identify potential sources of PM_{2.5} and PM₁₀ at the sampling site. PCA was used to identify the number of significant factors or sources contributing to the PM mass, which are characterized by specific tracers or pollution sources, whereas CA analysis verifies the relationship and difference between these elements as markers of different sources [3]. Meanwhile, Pearson correlation analysis establishes the inter-elemental relationships and identifies the rotations among the sources of PM. PCA and CA were completed using the Minitab 17 statistical software, while Pearson correlation analysis was performed with the ORIGIN 8 software.

PCA with varimax rotation was performed for compression of the data by reducing the number of variables from a large set of variables to a small set of uncorrelated variables called principal components that still contain most of the information in the large set. The first component accounts for the largest possible variance (variability in the data), and each succeeding component accounts for as much of the remaining variability as possible. The number of significant factors was based on the cumulative variance (>70%) and eigenvalue (must be greater than 1), Kaiser's criterion [21].

CA was performed to explore the set of homogeneous elemental clusters representing a particular receptor source. The process took place by dividing each metal into clusters. Subsequently, two or more metals with the highest similarity are combined until all elements are linked and are represented by a dendrogram source [3].

3. Results and Discussion

3.1. PM_{2.5} and PM₁₀ Mass Concentrations and Meteorology

Thailand's climate is influenced by two monsoons (the Southwest and Northeast monsoon) with three main seasons. The Southwest monsoon (from mid-May to September) usually brings warm and moist air from the Indian Ocean toward Thailand, resulting in abundant rain over the country. Meanwhile, the Northeast monsoon (from October to March) blows in from Indo-China, bringing relatively cool, dry conditions (less humidity and less chance of rainfall) to Thailand (except for the southern part of the country, where the rain blows in from the Pacific Ocean). In this dry period, haze events usually appear due to forest fires and the burning of agricultural residues. Three main seasons can be described as the following: the hot season (mid-February to mid-May), the wet season (mid-May to mid-October) and the cool season (mid-October to mid-February).

Temporal variations and summary statistics of meteorological parameters during the sampling period at Khlong Nueng station, Pathum Thani, located approximately 18 km from the motoring site, as recorded by the National Hydroinformatics Data Center, are shown in Figure 2 and Table 3, respectively. The maximum temperature ranged from 30.50 to 39.50 °C, and the highest maximum temperature was recorded during the pre-Southwest monsoon. Meanwhile, the minimum temperature was found to be from 20.5 to 29.0 °C and was highest during the Southwest monsoon. The average relative humidity was found to be 88.96%, while the maximum and minimum relative humidity were 70 and 98% in June and May, respectively (the Southwest monsoon). The maximum rainfall of 74.8 mm was

noted during the pre-Southwest monsoon, which was above normal. However, during the Southwest monsoon, the rainfall was below normal. The average wind speed was found to be 0.35 m/s, while the maximum wind speed was 2.50 m/s. The air pressure ranged from 754 to 763 mmHg with an average of 757 mmHg.

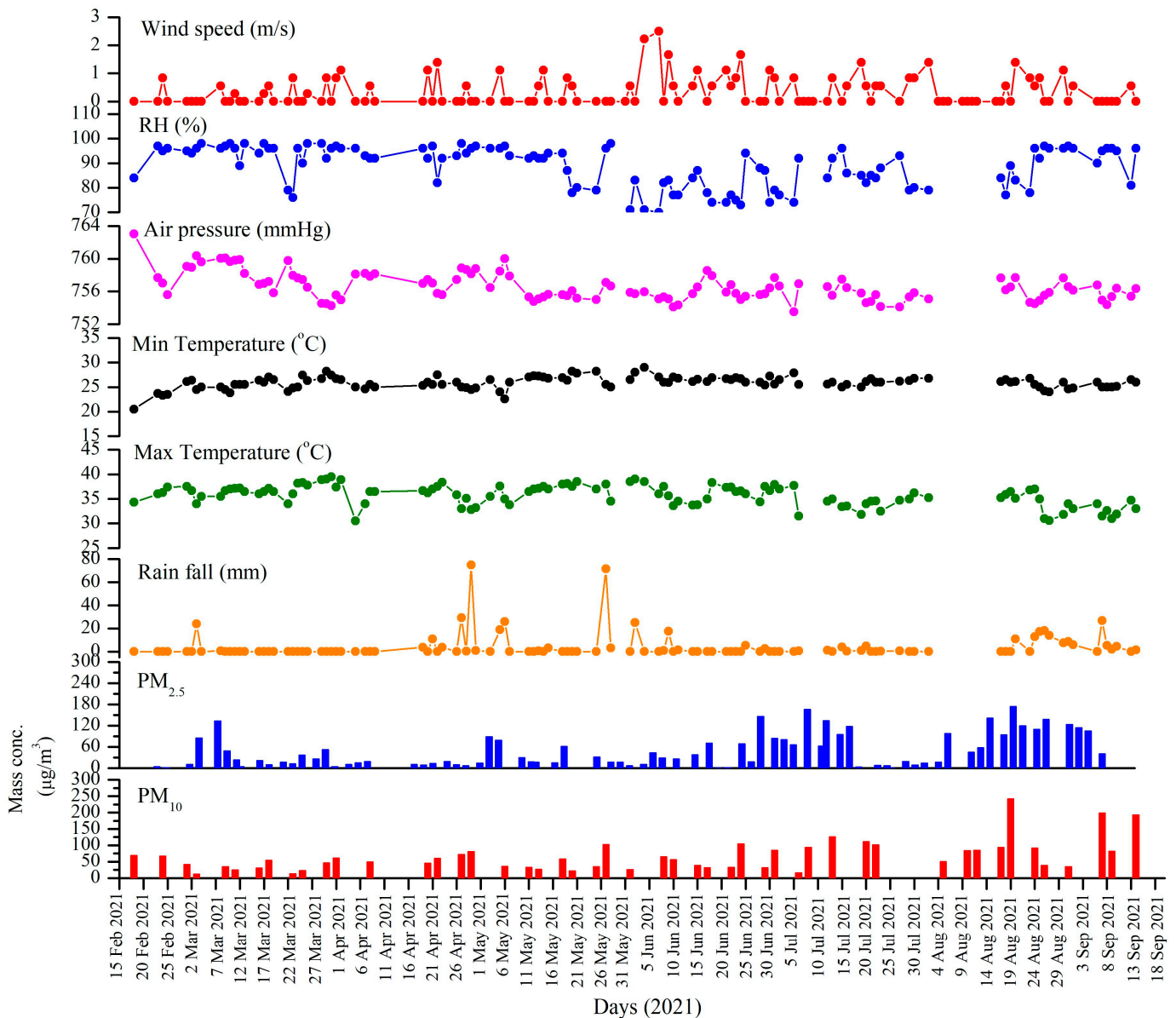


Figure 2. Temporal variations of $PM_{2.5}$ and PM_{10} mass concentrations and meteorological parameters (rainfall, maximum temperature, minimum temperature, air pressure, relative humidity and wind speed) at the Pathum Thani sampling site in the suburban area of Thailand from 18 February to 14 September 2021.

Figure 2 and Table 3 show the temporary variations and summary statistics of $PM_{2.5}$ and PM_{10} mass concentrations in suburban Pathum Thani, Thailand, during different seasons (summer and wet) from 18 February to 14 September 2021. Both 24-h monitoring $PM_{2.5}$ and PM_{10} levels in Pathum Thani were compared with three guideline levels for allowable 24-h $PM_{2.5}$ and PM_{10} concentrations, quoted from the World Health Organization (WHO), the United States Environmental Protection Agency (US EPA) and Thailand National Ambient Air Quality Standards (Thailand NAAQS). As can be seen in Figure 2, in summer days from mid-February to mid-May 2021, the maximum and minimum con-

concentrations of PM_{2.5} were 133.73 and 1.65 µg/m³, respectively, with an average value of 27.53 µg/m³ (n = 33), which was slightly higher than the WHO air quality guideline (25 µg/m³). However, this mean value was lower than the US EPA (35 µg/m³) and the NAAQS (50 µg/m³). Meanwhile, the maximum and minimum concentrations of PM₁₀ were 81.72 and 12.75 µg/m³, respectively, with an average value of 45.08 µg/m³ (n = 21). It can be noted that the mean concentration of PM₁₀ was below the values defined by the WHO (50 µg/m³), the US EPA (120 µg/m³) and the NAAQS (150 µg/m³).

Table 3. Summary statistics of PM_{2.5} and PM₁₀ mass concentration and meteorological parameters in Pathum Thani during the sampling period from 18 February to 14 September 2021.

Variable	Mean	Min	Max	SD
PM _{2.5} (µg/m ³)	48.10	0.39	174.26	46.97
PM ₁₀ (µg/m ³)	65.90	12.75	242.02	47.51
Rainfall (mm)	4.15	0.00	74.80	11.32
Min Temperature (°C)	25.88	20.50	29.00	1.24
Max Temperature (°C)	35.70	30.50	39.50	2.10
Air pressure (mmHg)	756.60	753.51	763.03	1.70
Relative humidity (%)	88.96	70.00	98.00	8.17
Wind speed (m/s)	0.35	0.00	2.50	0.52

In wet seasons (mid-May to September), the concentration of PM_{2.5} varied from 0.39 to 174.26 µg/m³ with an average value of 61.96 µg/m³ (n = 46). The mean concentration of PM_{2.5} in this season exceeded the values defined by the WHO, the US EPA and the NAAQS, while the concentration of PM₁₀ ranged from 16.06 to 242.02 µg/m³ with an average value of 81.51 µg/m³ (n = 28). The average concentration of PM₁₀ exceeded the value defined by the WHO; however, it was still below the values defined by the US EPA and the NAAQS. Normally, during the wet period in Thailand, PM_{2.5} and PM₁₀ concentrations are lower than in the summer and winter [22]. The mean concentration values of PM_{2.5} and PM₁₀ over the same (wet) period at Khlong Nueng station, Pathum Thani, located approximately 18 km from the motoring site, as reported by the PCD (<http://www.air4thai.com/webV2/history/> (accessed on 20 September 2021)) showed to be 11.81 and 30.62 µg/m³, which were lower than those obtained from our sampling site. The high mass concentrations of PM_{2.5} and PM₁₀ during the wet season might be due to the road and building construction activities near the monitoring site combined with low rainfall during this period (see Figure 2).

Table 4 shows the average concentrations of PM_{2.5} and PM₁₀ in several tropical countries. As shown in Table 4, the average concentration of PM_{2.5} in this study was higher than those in Chiang Mai [16], Jayapura, Indonesia [23] and Petaling Jaya, Malaysia [24]. However, it was much lower than those in Bangkok [12], which is the biggest urban site in Thailand. It was also significantly lower than those in Chiang Rai [10] and Pekanbaru, Indonesia [25]. Meanwhile, the average concentration of PM₁₀ in this study was much higher than those in Pekanbaru [25] and Jayapura, Indonesia [23], as well as Belisario Quito, Los Chillos and Tababela, Ecuador [26]. It can also be noted that the average concentration of PM₁₀ in this study was slightly higher than that of Barranquilla, Colombia [27].

Table 4. PM_{2.5} and PM₁₀ mass concentrations of this study and several tropical countries.

Study Area	Location Type	Sampling Period	PM Size Fraction	Average Conc. (µg/m ³)	References
Pathum Thani, Thailand	Suburban	Feb 2021–Sep 2021	PM _{2.5} PM ₁₀	48 ± 47 66 ± 48	This study
Bangkok, Thailand	Urban	Aug 2017–Mar 2018	PM _{2.5}	77 ± 21	[12]
Chiang Mai, Thailand	Urban	Jan 2017–Mar 2017	PM _{2.5}	36 ± 16	[16]
Chiang Rai, Thailand	Peri-urban	Jul 2021–Aug 2021	PM _{2.5}	63 ± 26	[10]
Pekanbaru, Indonesia	Urban	Apr 2014–Jul 2014	PM _{2.5} PM ₁₀	63 ± 3 28 ± 2	[25]
Jayapura, Indonesia	Suburban	Jan 2017–Dec 2017	PM _{2.5} PM ₁₀	6 ± 3 12 ± 3	[23]
Barranquilla, Colombia	Urban	Mar 2016–Apr 2016	PM ₁₀	52 ± 11	[27]
Belisario Quito, Ecuador	Urban	Jan 2017–Oct 2017	PM ₁₀	25 ± 9	[26]
Los Chillos, Ecuador	Industrial			26 ± 11	
Tababela, Ecuador	Peri-urban			26 ± 5	
Petaling Jaya, Malaysia	Suburban	Jan 2017–Feb 2018	PM _{2.5}	28 ± 10	[24]

3.2. Elemental Concentration

Table 5 presents the minimum, maximum and mean values, standard deviation (SD) and minimum detection limits (MDL) in ng/m³ for the elemental concentration in PM_{2.5} and PM₁₀ samples collected from Pathum Thani Province. For the PIXE technique, the detection limit highly depends on the presence of the other elements in the samples due to its impact on spectral interference. As a result, the detection limits vary from one sample to another [28]. The results showed that Fe, K, Cr and Ca (30–158 ng/m³) were the most abundant in PM_{2.5}. The second abundant was Zn, S, Ni, Si and Mn (15–21 ng/m³). Low concentrations were obtained for Cu, Ti and Cl (6–8 ng/m³). The relative contribution of Si, Fe, K, Ca, Mn and Ti was associated with crustal or natural origin. [29,30]. Meanwhile, Cr, Zn, S, Ni and Cu mostly originated from anthropogenic origin [7,29]. For PM₁₀, the crustal elements Fe, K, and Ca, ranging from 71–292 ng/m³, were in high concentrations, and the besides crustal elements, anthropogenic Cr and Ni, also had high concentrations (72–114 ng/m³). Anthropogenic (Zn, S, and Cu and Cl) and crustal (Si, Mn and Ti) elements were found in medium concentrations (10–25 ng/m³).

Table 5. Elemental concentrations of PM_{2.5} and PM₁₀ in Pathum Thani Province in ng/m³.

Element	MDL	PM _{2.5}				PM ₁₀			
		Mean	Min	Max	SD	Mean	Min	Max	SD
Si	0.31	17.90	1.08	72.67	17.50	15.18	1.67	57.71	12.94
S	0.26	20.86	0.71	107.92	21.13	17.70	1.44	50.05	14.42
Cl	0.24	6.63	0.48	30.25	6.26	15.44	1.20	86.20	17.27
K	0.66	74.79	1.23	355.01	73.81	70.79	10.07	220.67	51.69
Ca	1.17	30.71	1.51	137.64	28.78	139.13	29.18	485.94	90.23
Ti	0.22	7.04	0.30	125.04	17.88	10.51	0.92	37.60	8.42
Cr	0.57	65.43	1.44	948.16	163.74	113.59	0.75	1033.32	243.05
Mn	0.39	15.34	0.54	125.81	24.00	14.12	1.33	124.40	24.34
Fe	1.42	157.74	1.76	3879.18	491.03	291.82	22.42	4145.35	661.64
Zn	1.78	21.17	2.30	76.82	19.79	24.72	2.95	82.08	18.75
Ni	1.31	18.80	1.84	94.06	25.15	71.78	3.78	595.56	152.15
Cu	1.22	7.77	1.69	35.08	5.95	10.24	2.31	53.34	10.74

Significant changes in concentrations of key elements for PM_{2.5} and PM₁₀ during the whole period were observed, as shown in Figure 3. It can also be seen that Fe and Cr concentrations had similar temporal trends for both PM_{2.5} and PM₁₀. For PM_{2.5}, the seven concentration peaks of Fe and Cr occurred as follows: on 9 April, 30 April, 5 May, 19 May, 31 May, 30 June and 18 August at 3879, 872, 509, 1381, 521, 802 and 488 ng/m³ for Fe, and 948, 278, 156, 444, 179, 267 and 162 ng/m³ for Cr. For PM₁₀, the five concentration peaks of Fe and Cr occurred as follows: on 22 April, 13 May, 20 May, 1 June and 20 July at 4145, 893, 1225, 1121 and 1753 ng/m³ for Fe, and 1033, 246, 341, 330 and 490 ng/m³ for Cr.

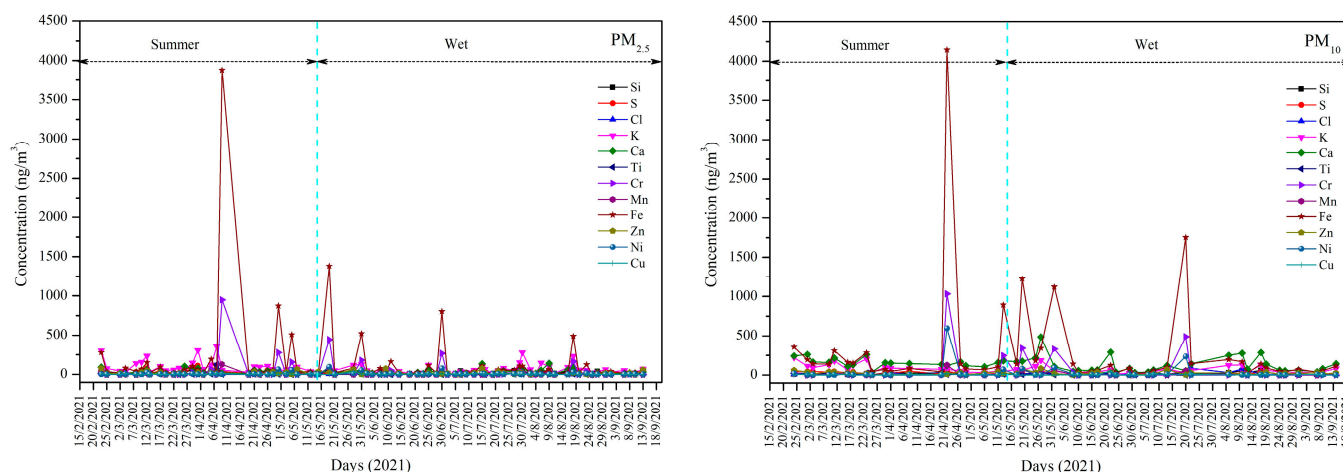


Figure 3. Variation of elements concentrations of PM_{2.5} and PM₁₀ samples over Pathum Thani Province from 18 February to 14 September 2021.

No significant pattern differences in element concentrations between summer and wet seasons for PM_{2.5} were observed, as shown in Figure 4. The mean concentrations of main elements for PM_{2.5}, such as Fe, K, Cr and S, in the summer season were significantly higher than those in the wet season. The concentrations of element species followed the order of Fe > K > Cr > S > Ca > Zn > Ni > Mn > Si > Ti > Cu > Cl for the summer season, and Fe > K > Cr > Ca > Zn > Ni > Si > Mn > S > Cu > Cl > Ti for the wet season. For PM₁₀, similar trends of element concentrations in the summer and wet seasons were noted (see Figure 4), and almost all element concentrations in the summer season were higher than those in the wet seasons, like in PM_{2.5}. The orders of element concentrations were Fe > Ca > Cr > Ni > K > Zn > S > Mn > Si > Cl > Ti > Cu for the summer season and Fe > Ca > Cr > K > Ni > Zn > Cl > Si > Mn > S > Cu > Ti for the wet season. A significantly lower element concentration in the wet season (monsoon) than in the summer season for both PM_{2.5} and PM₁₀ might be due to the metals being precipitated and washed out by frequent rain during the wet season [31].

3.3. Source Identification

3.3.1. Correlation Analysis

In order to identify qualitatively possible sources of PM_{2.5} and PM₁₀ contributing to the elements, Pearson's correlation analysis was performed. Pearson's correlation coefficient matrix relates the mass of PM_{2.5} and the elements concentrations of PM_{2.5}; the mass of PM₁₀ and the elements concentrations of PM₁₀ are given in Tables 6 and 7, respectively. As shown in Table 6, a weak correlation coefficient (r : 0.230–0.257) was found between the mass of PM_{2.5} and elements from crustal and biomass-burning origin such as Ca, K, Cl and S. Meanwhile, the correlation coefficient between the mass of PM₁₀ and elements was observed to be quite poor (r : 0.012–(−0.167)) (see Table 7). For the inter-elemental relationships of PM_{2.5}, it can be seen that the highest correlations were between Cr-Mn (r = 0.967), Cr-Fe (r = 0.990), Cr-Ni (r = 0.966), Mn-Fe (r = 0.949), Mn-Ni (r = 0.947) and Fe-Ni (r = 0.968). These strong correlations revealed that all of these

associated elements originated from road dust [32,33] and industrial emission sources; metallurgical, electromechanical, electronic industries and electroplating [34,35]. Fe, Mn and Cr are commonly used in the steel industry [7]. Cr and Ni are also often used in electroplating [7]. In addition, Zn releases from tire and brake abrasion as ZnO is used as a vulcanization agent to produce tires [33]. There were moderate positive correlations between Si-S ($r = 0.601$), Si-Ca ($r = 0.632$) and K-Ca ($r = 0.629$), Si-Cl ($r = 0.578$), Si-K ($r = 0.547$), which can be observed, suggesting they predominantly come from crustal sources [36]. Si classifies as clay, such as almandine or kaolinite, common in soils of tropical regions [19]. Ca and S are possibly from calcium sulfate. K and Ti are usually found in aluminosilicate clays. Cl can be absorbed from soil dust [19]. Subsequently, moderate positive correlations between S-K ($r = 0.741$) and Cl-K ($r = 0.614$), S-Cl ($r = 0.511$), S-Ca ($r = 0.577$) and Cl-Ca ($r = 0.556$), as well as a moderate negative correlation between K-Cr (-0.720), indicated that the source could be from biomass burning [37]. K and Cl are considered biomarkers for crop residue burning, such as wheat and rice [38]. K and Cl also probably relate to the use of fertilizers and herbicides in the field [39]. Meanwhile, S and Ca come from wood burning [40,41]. Moderate correlations between Zn-Cu ($r = 0.524$) and Mn-Cu ($r = 0.597$) involved vehicles exhaust [34,42] and industrial emission sources [43]. Another interesting correlation between Ti-Ni ($r = 0.725$) is probably attributed to industrial sources of different industrial types [44].

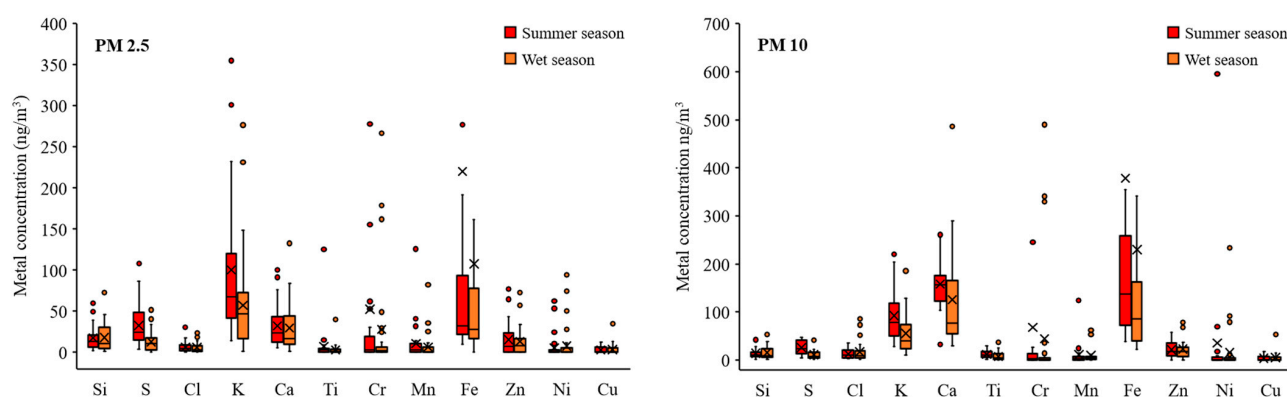


Figure 4. Metals concentration variations of PM_{2.5} and PM₁₀ in summer and wet seasons. The line in the box represents the median, the cross shows the mean values, the bottom and top of the vertical lines represent the values of the 5th and 95th percentiles, respectively, the dot denote the data beyond the mean values).

Table 6. Pearson’s correlation coefficients relating the mass of PM_{2.5} and the elements concentrations of PM_{2.5}.

	Mass	Si	S	Cl	K	Ca	Ti	Cr	Mn	Fe	Zn	Ni	Cu
Mass	1												
Si	−0.203	1											
S	−0.256	0.601	1										
Cl	−0.257	0.578	0.511	1									
K	−0.230	0.547	0.741	0.614	1								
Ca	−0.252	0.632	0.577	0.556	0.629	1							
Ti	−0.152	0.029	0.064	0.210	0.492	0.189	1						
Cr	−0.157	0.037	−0.009	−0.146	−0.720	−0.018	0.301	1					
Mn	−0.207	0.033	0.063	−0.059	0.039	0.073	0.444	0.967	1				
Fe	−0.140	0.123	0.088	−0.042	0.003	0.024	0.041	0.990	0.949	1			
Zn	−0.011	−0.007	0.262	0.209	0.230	0.384	−0.117	−0.153	−0.062	−0.085	1		
Ni	−0.081	−0.239	−0.117	−0.286	−0.112	−0.008	0.725	0.966	0.947	0.968	−0.117	1	
Cu	−0.025	0.094	0.212	0.175	0.194	0.202	0.094	0.099	0.597	0.133	0.524	−0.021	1

Shaded correlation coefficients are statistically significant at $p < 0.05$.

Table 7. Pearson’s correlation coefficients relating the mass of PM₁₀ and the elements concentrations of PM₁₀.

	Mass	Si	S	Cl	K	Ca	Ti	Cr	Mn	Fe	Zn	Ni	Cu
Mass	1												
Si	0.071	1											
S	−0.167	0.508	1										
Cl	0.012	0.480	0.252	1									
K	−0.107	0.393	0.737	0.259	1								
Ca	−0.065	0.625	0.685	0.386	0.804	1							
Ti	−0.140	0.265	0.367	0.213	0.535	0.520	1						
Cr	0.151	0.354	0.187	−0.022	−0.182	−0.149	−0.181	1					
Mn	−0.080	0.297	0.189	−0.031	−0.024	−0.031	−0.168	0.971	1				
Fe	−0.059	0.367	0.261	0.015	0.021	0.030	−0.052	0.993	0.970	1			
Zn	0.084	−0.037	0.296	0.005	0.383	0.484	0.090	−0.050	0.028	−0.008	1		
Ni	0.041	0.696	0.371	0.021	−0.146	−0.209	−0.206	0.969	0.914	0.984	−0.306	1	
Cu	−0.167	0.279	0.176	0.121	0.077	0.441	0.274	0.746	0.125	0.145	0.204	0.049	1

Shaded correlation coefficients are statistically significant at $p < 0.05$.

As can be seen in Table 7, for the inter-elemental relationships of PM₁₀, Cr showed strong positive correlations with Mn ($r = 0.971$), Fe ($r = 0.993$), Ni ($r = 0.969$) and Cu ($r = 0.746$). Mn also displayed important correlations with Fe ($r = 0.970$) and Ni ($r = 0.914$). A strong correlation between Fe-Ni ($r = 0.984$) can be noted. These highest correlations were quite similar to PM_{2.5} and had similar source origin from road dust and industrial emission. Vaio et al. (2016) [45] discovered that Cr and Cu contained in PM₁₀ can be attributed to industrial sources. Ahmad et al. (2022) [13] also reported that Mn and Ni may result from industrial emissions, while Cu and Cr originated from road dust. Truong et al. (2022) [46] found that Cr, Ni, Fe and Cu related to non-ferrous metallurgical industry, metal processing and refinery industry emissions. Meanwhile, Si was well correlated with Ca ($r = 0.625$) and had moderate correlations with S ($r = 0.508$). K also showed a strong correlation with Ca ($r = 0.804$) and a moderate correlation with Ti ($r = 0.535$). Ca displayed a moderate correlation with Ti ($r = 0.520$). This observation suggested that all of these associated elements were mainly from crustal sources [27]. Good correlations between S-K ($r = 0.737$) and S-Ca ($r = 0.685$) were noted, suggesting a possible contribution of biomass burning [47]. Another interesting correlation was Si-Ni ($r = 0.696$), which revealed that it possibly originated from industrial sources such as metallurgical processes [40] and steel industries [26].

As for the correlation analysis results of PM_{2.5} and PM₁₀, the emission sources of PM_{2.5} and PM₁₀ were quite similar. The main emission sources related to road dust and industrial, crustal and biomass burning. These sources are associated with the combination of several activities of the monitoring site, which comprises many large and medium-scale industries such as metallurgical, electromechanical, electronic industries and electroplating, as well as a significant number of commercial centers, agricultural land and residential areas.

3.3.2. PCA Analysis

PCA was employed to predict the potential sources of PM_{2.5} and PM₁₀. The PCA results are summarized in Table 8, and the possible sources of PM_{2.5} and PM₁₀, as identified using PCA, are shown in Figure 5. The obtained results for both PM_{2.5} and PM₁₀ were in agreement with the inter-element relationships obtained from Pearson’s correlation matrix results. As can be seen in Table 8, PCA resolved four components explaining 76.7% cumulative variance for PM_{2.5}. The strongest Factor 1 explained 32.4% of the total variance with an eigenvalue of 3.89. The influenced element consisted of Si, S, Cl, K and Ca. The elements such as Si, K and Ca may be from the local soil dust. Bangar et al. (2021) [48] and Onat et al. (2013) [49] reported that crustal dust (soil and surface dust) is the primary source of Si, K and Ca. Potassium (K), chlorine (Cl) and sulfur (S) were considered tracers of agricultural-residue (biomass) burning [34,47,48]. The area of Pathum Thani is mostly

surrounded by rice paddy fields. Rice paddies are burned after the harvesting season from November to April. Therefore, this factor should be identified as a combined soil/surface dust and biomass burning.

Table 8. Summary of principal component analysis (PCA) of elements in PM_{2.5} and PM₁₀ in Pathum Thani Province.

Element	PM _{2.5}				PM ₁₀		
	Factor 1	Factor 2	Factor 3	Factor 4	Factor 1	Factor 2	Factor 3
Si	0.831	0.123	−0.052	0.109	0.305	0.370	−0.719
S	0.843	0.081	0.14	0.047	0.219	0.790	−0.222
Cl	0.724	−0.049	0.033	−0.181	−0.087	0.171	−0.743
K	0.794	−0.006	0.181	−0.413	−0.040	0.914	−0.098
Ca	0.807	0.040	0.186	−0.106	−0.054	0.858	−0.380
Ti	0.172	0.085	0.058	−0.952	−0.149	0.646	−0.223
Cr	0.002	0.985	0.045	0.024	0.990	−0.052	−0.085
Mn	0.134	0.972	0.057	−0.005	0.969	0.059	−0.051
Fe	0.012	0.954	0.097	0.053	0.989	0.047	−0.099
Zn	0.242	−0.049	0.792	0.083	0.038	0.695	0.178
Ni	0.025	0.637	−0.098	−0.169	0.973	−0.057	−0.117
Cu	0.028	0.094	0.817	−0.155	0.162	−0.006	−0.625
EV	3.886	3.039	1.227	1.050	4.351	3.551	1.199
V (%)	32.4	25.3	10.2	8.7	36.3	29.6	10.0
CV (%)	32.4	57.7	67.9	76.7	36.3	65.8	75.8

EV = eigenvalue; V = variance contribution rate (%); CV = cumulative variance (%).

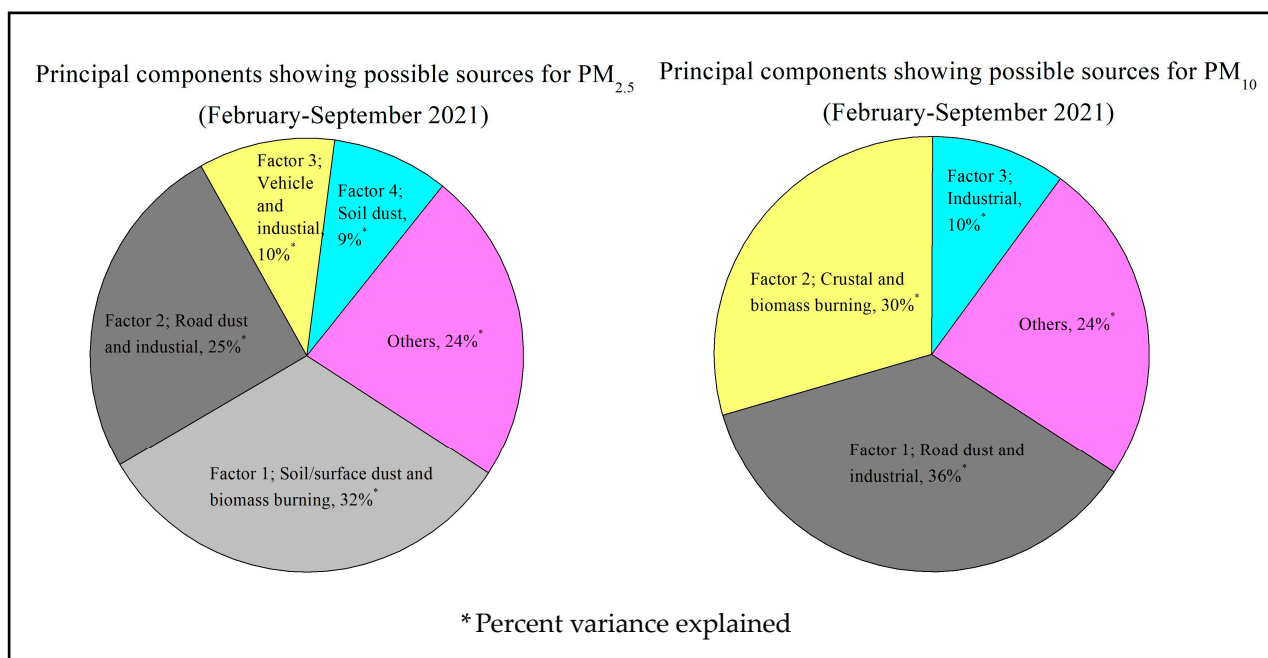


Figure 5. Source identification of PM_{2.5} and PM₁₀ derived from PCA analysis over Pathum Thani area during February–September 2021.

Factor 2 accounted for 25.3% of the total variance with an eigenvalue of 3.04. It strongly correlated with Mn, Fe, Cr and Ni. This represented a mixture of road dust and industrial emission sources [50]. Mn, Fe and Cr are fingerprint elements for road dust sources [49]. Bie et al. (2021) [50] reported that Mn, Fe and Cr are the main chemical components in profiles of industrial emission. Wang et al. (2019) [7] reported that Cr and Ni are emitted from industrial sources such as chemical, metallurgical, electromechanical, and electronic

industries. There is a large industrial zone composed of various industries, such as metal processing, steel wires and electronic power equipment, located approximately 20 km northwest of the monitoring site.

Factor 3 explained 10.2% of the total variance with Zn and Cu as the main elements. Zn and Cu are commonly recognized as a source of the mechanical wear of motor vehicles and tire wear [7]. Ahmad et al. (2020) [51] reported that Zn and Cu might have originated from the oil-based combustion industry. Therefore, a plausible source for Factor 3 would be a combined vehicle exhaust and industrial emission [50].

Factor 4 accounted for 8.7% of the total variance, and it was mainly made up of Ti. Ti most likely originated from soil dust [19]. This factor was likely a soil dust source.

In the PCA analysis of PM₁₀, three factors explained 75.8% of the total variance. Factor 1 showed high loading of Mn, Fe, Cr and Ni, and it accounted for 33.6% of the total variance. It was assigned to a mixed resuspended road dust and industrial emission very similar to PM_{2.5} Factor 2. The elements such as Mn, Fe and Cr are the main elements in road dust [52,53]. Cr and Ni may be associated with the various industrial activities [26,54] located approximately 20 km northwest of the monitoring site, such as metal processing, steel wires and electronic power equipment. Cr and Ni are emitted from the combustion process and metallurgical industries [52,55].

Factor 2 explained 29.6% of the total variance and was dominated by S, K, Ca, Ti and Zn. Elements such as K, Ca, Ti and Zn could be attributed to crustal dust [6]. The presence of S and K indicated the contribution of biomass burning [44]. Factor 2 can therefore be identified as a mixture of crustal dust and a biomass-burning source similar to PM_{2.5} Factor 1.

Factor 3 explained 10.0% of the total variance, and it was characterized by Si, Cl and Cu. Si and Cl might be from the industrial coal combustion process [54]. Panda and Nagendra (2018) [31] reported that Cu can be emitted from industrial combustion processes and metal industries. Therefore, this Factor may originate from industrial sources.

3.3.3. CA Analysis

The CA was also calculated to support the PCA results, as shown in Figure 6. Figure 6 shows that the grouping obtained with the CA analysis was in good agreement with the PCA results for both PM_{2.5} and PM₁₀. For PM_{2.5}, the first group was characterized by a group of elements with Si, S, Ca, Cl and K, which was very similar to Factor 1 of PCA, representing soil dust with a significant contribution to biomass burning. The second cluster included Cr, Fe, Mn and Ni and matched well with Factor 2 of PCA, indicating road dust combined with industrial emission. The third group showed a link between Zn and Cu analogous to Factor 3 of PCA. The possible sources were vehicle exhaust and some contributions from industrial emissions. The last group characterized by CA was Ti, which appeared on its own and was not linked to any elements. Ti is a marker element for crustal dust. This result was consistent with Factor 4 of PCA.

The dendrogram of the CA analysis for PM₁₀ is shown in Figure 7. The first cluster with elements such as Si, Cl and Cu represented the industrial emission. This was in good agreement with Factor 3 of PCA. The second cluster showed a group of elements such as Cr, Ni, Mn and Fe. This was absolutely in agreement with Factor 1 of PCA and represented a mixed source related to anthropogenic activities, including road dust and industrial emissions. The third cluster was a link between S, K, Ca, Ti and Zn and similar to Factor 2 of PCA. The presence of these elements can be attributed to crustal dust (K, Ca, Ti and Zn) together with the source of biomass burning (S and K).

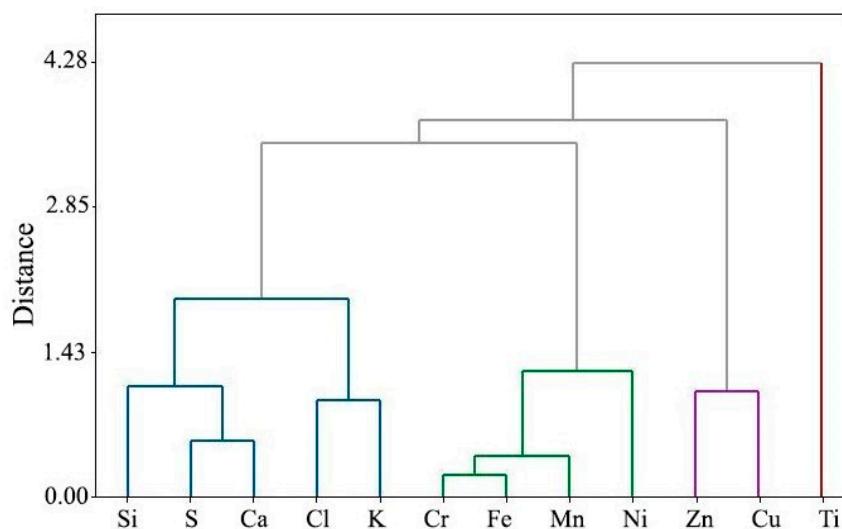


Figure 6. Dendrogram of the cluster analysis for PM_{2.5}.

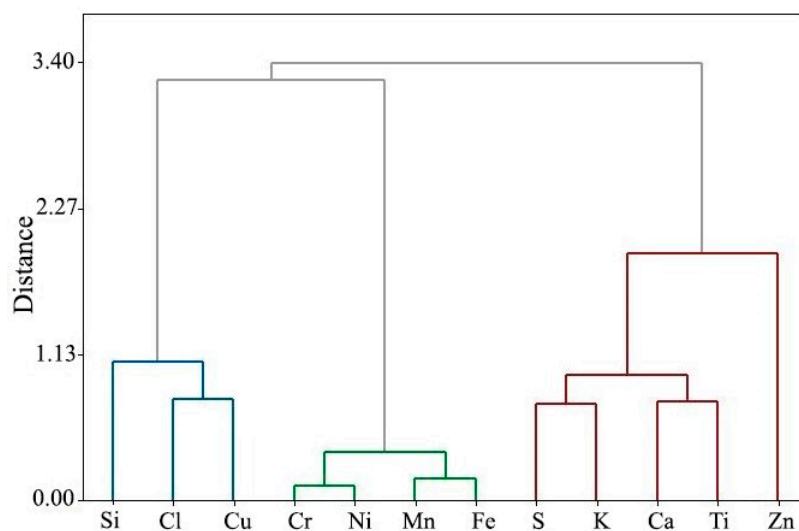


Figure 7. Dendrogram of the cluster analysis for PM₁₀.

It can be concluded from the CA analysis results that the major pollution sources of both PM_{2.5} and PM₁₀ were quite similar. There were four main sources of biomass burning, a mix of road dust and industrial emission, vehicle exhaust and industrial emission, and crustal dust contained in PM_{2.5}. Meanwhile, for PM₁₀, there were three main contributory pollution sources, and these were industrial emission, a mix of road dust and industrial emission and a mix of crustal dust and biomass burning.

4. Conclusions

In this work, the elemental characterization and source identification of PM_{2.5} and PM₁₀ at a suburban site in Thailand during summer and wet seasons from 18 February 2021 to 14 September 2021 was performed. The results showed that the annual mean concentrations of PM_{2.5} and PM₁₀ were $48.10 \pm 46.97 \mu\text{g}/\text{m}^3$ and $65.90 \pm 47.51 \mu\text{g}/\text{m}^3$, respectively. It can be observed that the concentration of PM_{2.5} in the wet season, with a mean value of $61.96 \mu\text{g}/\text{m}^3$ was higher than the NAAQS. The elements concentration in PM_{2.5} were in descending order as follows: Fe > K > Cr > Ca > Zn > S > Ni > Si > Mn > Cu > Ti > Cl, while the order of elements concentration for PM₁₀ was Fe > Ca > Cr > Ni > K > Zn > S > Cl > Si > Mn > Ti > Cu. The high concentrations of Fe, K, Cr, Ni and Ca indicated that they originated from industrial sources, except for K and Ca, which could be

soil dust but could also be emitted from biomass burning. A significant seasonal variation in elemental concentrations of PM_{2.5} and PM₁₀ was observed, with their highest values during the summer season followed by the wet season. The source identification using PCA was influenced by four and three possible factors for PM_{2.5} and PM₁₀, respectively. The identified sources for PM_{2.5} were soil dust and biomass burning, road dust and industrial emission, vehicle and industrial emission and soil dust, respectively. In the case of PM₁₀, the possible sources were road dust and industrial emission, crustal and biomass burning and industrial sources, respectively. These results were also confirmed by the CA and correlation analysis data.

Author Contributions: S.N.: Investigation, methodology, data curation; W.K.: Formal analysis, data curation, visualization; U.T.: validation, resources, investigation; W.S.: Validation, resources, investigation; R.F.: Investigation, resources; D.R.: Conceptualization, funding acquisition, writing—original draft, writing—review and editing. All authors have read and agreed to the published version of the manuscript.

Funding: This research is funded by the Regional Office of the Regional Cooperative Agreement for Research, Development and Training related to Nuclear Science and Technology for Asia and the Pacific (RCARO) (Contract No.: RCARP02/RC08) and the National Research Council of Thailand (NRCT). This work was also supported in part by the International Atomic Energy Agency (IAEA) 2022–2025 Technical Cooperation Programme, THA0016.

Data Availability Statement: Data will be available by request to the corresponding authors.

Conflicts of Interest: The authors declare no conflict of interest. The funders had no role in the design of the study; in the collection, analyses, or interpretation of data; in the writing of the manuscript; or in the decision to publish the results.

References

1. Diapouli, E.; Fetfatzis, P.; Panteliadis, P.; Spitiieri, C.; Gini, M.I.; Papagiannis, S.; Vasilatou, V.; Eleftheriadis, K. PM_{2.5} source apportionment and implications for particle hygroscopicity at an urban background site in Athens, Greece. *Atmosphere* **2022**, *13*, 1685. [[CrossRef](#)]
2. Zhang, G.; Ding, C.; Jiang, K.; Pan, G.; Wei, X.; Sun, Y. Chemical compositions and sources contribution of atmospheric particles at a typical steel industrial urban site. *Sci. Rep.* **2020**, *10*, 7654. [[CrossRef](#)] [[PubMed](#)]
3. Waheed, S.; Jaafar, M.Z.; Siddique, N.; Markwitz, A.; Brereton, R.G. PIXE analysis of PM_{2.5} and PM_{2.5–10} for air quality assessment of Islamabad, Pakistan: Application of chemometrics for source identification. *J. Environ. Sci. Health Part A* **2012**, *47*, 2016–2027. [[CrossRef](#)] [[PubMed](#)]
4. Dong, D.; Qiu, T.; Du, S.; Gu, Y.; Li, A.; Hua, X.; Ning, Y.; Liang, D. The chemical characterization and source apportionment of PM_{2.5} and PM₁₀ in a typical city of Northeast China. *Urban Clim.* **2023**, *47*, 101373. [[CrossRef](#)]
5. Usman, F.; Zeb, B.; Alam, K.; Valipour, M.; Ditta, A.; Sorooshian, A.; Roy, R.; Ahmad, I.; Iqbal, R. Exploring the mass concentration of particulate matter and its relationship with meteorological parameters in the Hindu-Kush Range. *Atmosphere* **2022**, *13*, 1628. [[CrossRef](#)]
6. Ramírez, O.; Campa, A.M.S.; Amato, F.; Ruth, A.; Catacolí, R.A.; Rojas, N.Y.; Rosa, J. Chemical composition and source apportionment of PM at an urban background site in a high-altitude Latin American megacity (Bogota, Colombia). *Environ. Pollut.* **2018**, *233*, 142–155. [[CrossRef](#)]
7. Wang, S.; Yu, R.; Shen, H.; Wang, S.; Hu, Q.; Cui, J.; Yan, Y.; Huang, H.; Hu, G. Chemical characteristics, sources, and formation mechanisms of PM_{2.5} before and during the Spring Festival in a coastal city in Southeast China. *Environ. Pollut.* **2019**, *251*, 442–452. [[CrossRef](#)]
8. Kanjanasiranont, N.; Butburee, T.; Peerakiatkhajohn, P. Characteristics of PM₁₀ levels monitored in Bangkok and its vicinity areas, Thailand. *Atmosphere* **2022**, *13*, 239. [[CrossRef](#)]
9. Kliengchuay, W.; Srimanus, W.; Srimanus, R.; Kiangkoo, N.; Moonsri, K.; Niampradit, S.; Suwanmanee, S.; Tantrakarnapa, K. The association of meteorological parameters and AirQ+ health risk assessment of PM_{2.5} in Ratchaburi province, Thailand. *Sci. Rep.* **2022**, *12*, 12971. [[CrossRef](#)]
10. Niampradit, S.; Kliengchuay, W.; Mingkhwan, R.; Worakhunpiset, S.; Kiangkoo, N.; Suntorn, S.; Hongthong, A.; Siriratruengsuk, W.; Muangsuwan, T.; Tantrakarnapa, K. The elemental characteristics and human health risk of PM_{2.5} during haze episode and non-haze episode in Chiang Rai Province, Thailand. *Int. J. Environ. Res. Public Health* **2022**, *19*, 6127. [[CrossRef](#)]
11. Kayee, J.; Sompongchaiyakul, P.; Sanwlani, N.; Bureekul, S.; Wang, X.; Das, R. Metal concentrations and source apportionment of PM_{2.5} in Chiang Rai and Bangkok, Thailand during a biomass burning season. *ACS Earth Space Chem.* **2020**, *4*, 1213–1226. [[CrossRef](#)]

12. ChooChuay, C.; Pongpiachan, S.; Tipmanee, D.; Suttinun, O.; Deelaman, W.; Wang, Q.; Xing, L.; Li, G.; Han, Y.; Palakun, J.; et al. Impacts of PM_{2.5} sources on variations in particulate chemical compounds in ambient air of Bangkok, Thailand. *Atmos. Pollut. Res.* **2020**, *11*, 1657–1667. [[CrossRef](#)]
13. Ahmad, M.; Manjantrarat, T.; Rattanawongsa, W.; Muenri, P.; Saenmuangchin, R.; Klamchuen, A.; Aueviriyavit, S.; Sukrak, K.; Kangwansupamonkon, W.; Panyametheekul, S. Chemical composition, sources, and health risk assessment of PM_{2.5} and PM₁₀ in urban sites of Bangkok, Thailand. *Int. J. Environ. Res. Public Health* **2022**, *19*, 14281. [[CrossRef](#)] [[PubMed](#)]
14. Johnston, H.J.; Mueller, W.; Steinle, S.; Vardoulakis, S.; Tantrakarnapa, K.; Loh, M.; Cherrie, J.W. How harmful is particulate matter emitted from biomass burning? A Thailand perspective. *Curr. Pollut. Rep.* **2019**, *5*, 353–377. [[CrossRef](#)]
15. Vongruang, P.; Pimonsree, S. Biomass burning sources and their contributions to PM₁₀ concentrations over countries in mainland Southeast Asia during a smog episode. *Atmos. Environ.* **2020**, *228*, 117414. [[CrossRef](#)]
16. Kawichai, S.; Prapamontol, T.; Cao, F.; Song, W.; Zhang, Y. Source identification of PM_{2.5} during a smoke haze period in Chiang Mai, Thailand, using stable carbon and nitrogen isotopes. *Atmosphere* **2022**, *14*, 1149. [[CrossRef](#)]
17. Peng-in, B.; Sanitlua, P.; Monjatturat, P.; Boonkerd, P.; Phosri, A. Estimating ground-level PM_{2.5} over Bangkok Metropolitan Region in Thailand using aerosol optical depth retrieved by MODIS. *Air Qual. Atmos. Health* **2022**, *15*, 2091–2102. [[CrossRef](#)] [[PubMed](#)]
18. Wimolwatanapu, W.; Hopke, P.K.; Pongkiatkul, P. Source apportionment and potential source locations of PM_{2.5} and PM_{2.5–10} at residential sites in metropolitan Bangkok. *Atmos. Pollut. Res.* **2011**, *2*, 172–181. [[CrossRef](#)]
19. Rincon, G.; Quintana, G.M.; Gonzalez, A.; Buitrago, Y.; Gonzalez, J.C.; Molina, C.; Jones, B. PM_{2.5} exceedances and source appointment as inputs for an early warning system. *Environ. Geochem. Health* **2022**, *44*, 4569–4593. [[CrossRef](#)]
20. Cohen, D.D.; Bailey, G.M.; Kondepudi, R. Elemental analysis by PIXE and other IBA techniques and their application to source fingerprinting of atmospheric fine particle pollution. *Nucl. Instrum. Methods Phys. Res. Sect. B* **1996**, *109–110*, 218–226. [[CrossRef](#)]
21. De La Cruz, A.H.; Roca, Y.B.; Suarez-Salas, L.; Pomalaya, J.; Tolentino, D.A.; Gioda, A. Chemical characterization of PM_{2.5} at rural and urban sites around the Metropolitan area of Huancayo (Central Andes of Peru). *Atmosphere* **2019**, *10*, 21. [[CrossRef](#)]
22. Kanchanasuta, S.; Sooktawee, S.; Patpai, A.; Vatanasomboon, P. Temporal Variations and Potential Source Areas of Fine Particulate Matter in Bangkok, Thailand. *Air Soil Water Res.* **2020**, *13*, 1–10. [[CrossRef](#)]
23. Santoso, M.; Lestiani, D.D.; Kurniawati, S.; Damastuti, E.; Kusmartini, I.; Atmodjo, D.P.D.; Sari, D.K.; Hopke, P.K.; Mukhtar, R.; Muhtarom, T.; et al. Assessment of urban air quality in Indonesia. *Aerosol Air Qual. Res.* **2020**, *20*, 2142–2158. [[CrossRef](#)]
24. Hassan, H.; Latif, M.T.; Juneng, L.; Amil, N.; Khan, M.F.; Fujii, Y.; Jamhari, A.A.; Hamid, H.H.A.; Banerjee, T. Chemical characterization and sources identification of PM_{2.5} in a tropical urban city during non-hazy conditions. *Urban Clim.* **2021**, *39*, 100953. [[CrossRef](#)]
25. Siregar, S.; Idiawati, N.; Lestari, P.; Berekute, A.K.; Pan, W.; Yu, K. Chemical composition, source appointment and health risk of PM_{2.5} and PM_{2.5–10} during forest and peatland fires in Riau, Indonesia. *Aerosol Air Qual. Res.* **2022**, *22*, 220015. [[CrossRef](#)]
26. Zalakeviciute, R.; Rybarczyk, Y.; Granda-Albuja, M.G.; Suarez, M.V.D.; Alexandrino, K. Chemical characterization of urban PM₁₀ in the Tropical Andes. *Atmos. Pollut. Res.* **2020**, *11*, 343–356. [[CrossRef](#)]
27. Gómez-Plata, L.; Agudelo-Castañeda, D.; Castell, M.; Teixeira, E.C. PM₁₀ source identification: A case of a coastal city in Colombia. *Aerosol Air Qual. Res.* **2022**, *22*, 210293. [[CrossRef](#)]
28. Lestiani, D.D.; Santoso, M. Analytical methods INAA and PIXE applied to characterization of airborne particulate matter in Bandung, Indonesia. *At. Indones.* **2011**, *37*, 52–56. [[CrossRef](#)]
29. Zhang, T.; Su, Y.; Deboz, J.; Noble, M.; Munoz, A.; Xu, X. Continuous measurements, and source apportionment of ambient PM_{2.5}-bound elements in Windsor, Canada. *Atmosphere* **2023**, *14*, 374. [[CrossRef](#)]
30. Shaltout, A.A.; Boman, J.; Hassan, S.K.; Abozied, A.M.; Al-Ashkar, E.A.; Abd-Elkader, O.H.; Yassin, M.A.; Al-Tamimi, J.H. Elemental composition of PM_{2.5} aerosol in a residential–industrial area of a Mediterranean Megacity. *Arch. Environ. Contam. Toxicol.* **2020**, *78*, 68–78. [[CrossRef](#)]
31. Panda, S.; Nagendra, S.M.S. Chemical and morphological characterization of respirable suspended particulate matter (PM₁₀) and associated health risk at a critically polluted industrial cluster. *Atmos. Pollut. Res.* **2018**, *9*, 791–803. [[CrossRef](#)]
32. Wiseman, C.L.S.; Levesque, C.; Rasmussen, P.E. Characterizing the sources, concentrations and resuspension potential of metals and metalloids in the thoracic fraction of urban road dust. *Sci. Total Environ.* **2021**, *786*, 147467. [[CrossRef](#)] [[PubMed](#)]
33. Samek, L.; Stegowski, Z.; Styszko, K.; Furman, L.; Zimnoch, M.; Skiba, A.; Kistler, M.; Kasper-Giebl, A.; Rozanski, K.; Konduracka, E. Seasonal variations of chemical composition of PM_{2.5} fraction in the urban area of Krakow, Poland: PMF source attribution. *Air Qual. Atmos. Health* **2020**, *13*, 89–96. [[CrossRef](#)]
34. Gope, M.; Masto, R.E.; George, J.; Balachandran, S. Tracing source, distribution and health risk of potentially harmful elements (PHEs) in street dust of Durgapur, India. *Ecotoxicol. Environ. Saf.* **2018**, *154*, 280–293. [[CrossRef](#)] [[PubMed](#)]
35. Wang, Y.; Zhang, Y.; Li, X.; Cao, J. Refined source apportionment of atmospheric PM_{2.5} in a Typical City in Northwest China. *Aerosol Air Qual. Res.* **2021**, *21*, 200146. [[CrossRef](#)]
36. Evagelopoulos, V.; Begou, P.; Zoras, S. In-depth study of PM_{2.5} and PM₁₀ concentrations over a 12-year period and their elemental composition in the Lignite Center of Western Macedonia, Greece. *Atmosphere* **2022**, *13*, 1900. [[CrossRef](#)]
37. Rahman, M.S.; Bhuiyan, S.S.; Ahmed, Z.; Saha, N.; Begum, B.A. Characterization and source apportionment of elemental species in PM_{2.5} with especial emphasis on seasonal variation in the capital city “Dhaka”, Bangladesh. *Urban Clim.* **2021**, *36*, 100804. [[CrossRef](#)]

38. Saggi, G.S.; Mittal, S.K. Source apportionment of PM₁₀ by positive matrix factorization model at a source region of biomass burning. *J. Environ. Manag.* **2020**, *266*, 110545. [[CrossRef](#)] [[PubMed](#)]
39. Sillapapiromsuk, S.; Chantara, S.; Tengjaroenkul, U.; Prasitwattanaseree, S.; Prapamontol, T. Determination of PM₁₀ and its ion composition emitted from biomass burning in the chamber for estimation of open burning emissions. *Chemosphere* **2013**, *93*, 1912–1919. [[CrossRef](#)]
40. Popouen, A.J.; Benchrif, A.; Kezo, P.C.; Agbo, D.D.A.; Koua, A.A.; Bounakhla, M.; Monnehan, A.G. Elemental Composition of PM_{2.5} and PM₁₀ in the Industrial Area of Yopougon, Abidjan, Côte d'Ivoire. *J. Environ. Prot.* **2022**, *13*, 385–397. [[CrossRef](#)]
41. Molnár, P.; Gustafson, P.; Johannesson, S.; Boman, J.; Barregård, L.; Sällstena, G. Domestic wood burning and PM_{2.5} trace elements: Personal exposures, indoor and outdoor levels. *Atmos. Environ.* **2005**, *39*, 2643–2653. [[CrossRef](#)]
42. Xia, L.; Gao, Y. Characterization of trace elements in PM_{2.5} aerosols in the vicinity of highways in northeast New Jersey in the U.S. east coast. *Atmos. Pollut. Res.* **2011**, *2*, 34–44. [[CrossRef](#)]
43. Juda-Rezler, K.; Reizer, M.; Maciejewska, K.; Błaszczak, B.; Klejnowski, K. Characterization of atmospheric PM_{2.5} sources at a Central European urban background site. *Sci. Total Environ.* **2020**, *713*, 136729. [[CrossRef](#)] [[PubMed](#)]
44. Khan, J.Z.; Sun, L.; Tian, Y.; Shi, G.; Feng, Y. Chemical characterization and source apportionment of PM₁ and PM_{2.5} in Tianjin, China: Impacts of biomass burning and primary biogenic sources. *J. Environ. Sci.* **2021**, *99*, 196–209. [[CrossRef](#)] [[PubMed](#)]
45. Vaio, P.D.; Magli, E.; Barbato, F.; Caliendo, G.; Coccoziello, B.; Corvino, A.; Marco, A.D.; Fiorino, F.; Frecentese, F.; Onorati, G.; et al. Chemical composition of PM₁₀ at urban sites in Naples (Italy). *Atmosphere* **2016**, *7*, 163. [[CrossRef](#)]
46. Truong, M.T.; Nguyen, L.S.P.; Hien, T.T.; Pham, T.D.H.; Do, T.T.L. Source apportionment and risk estimation of heavy metals in PM₁₀ at a Southern Vietnam megacity. *Aerosol Air Qual. Res.* **2022**, *22*, 220094. [[CrossRef](#)]
47. Deng, J.; Jiang, L.; Miao, W.; Zhang, J.; Dong, G.; Liu, K.; Chen, J.; Peng, T.; Fu, Y.; Ahou, Y.; et al. Characteristics of fine particulate matter (PM_{2.5}) at Jinsha Site Museum, Chengdu, China. *Environ. Sci. Pollut. Res.* **2022**, *29*, 1173–1183. [[CrossRef](#)]
48. Bangar, V.; Mishra, A.K.; Jangid, M.; Rajput, P. Elemental Characteristics and source-apportionment of PM_{2.5} during the post-monsoon season in Delhi, India. *Front. Sustain. Cities* **2021**, *3*, 648551. [[CrossRef](#)]
49. Onat, B.; Sahin, U.A.; Akyuz, T. Elemental characterization of PM_{2.5} and PM₁ in dense traffic area in Istanbul, Turkey. *Atmos. Pollut. Res.* **2013**, *4*, 101–105. [[CrossRef](#)]
50. Bie, S.; Yang, L.; Zhang, Y.; Huang, Q.; Li, J.; Zhao, T.; Zhang, X.; Wanga, P.; Wang, W. Source appointment of PM_{2.5} in Qingdao Port, East of China. *Sci. Total Environ.* **2021**, *755*, 142456. [[CrossRef](#)]
51. Ahmad, M.; Rihawy, M.S.; Haydr, R.; Tlass, M.; Roumie, M.; Srouf, A. PIXE and statistical analysis of fine airborne particulate matter (PM_{2.5}) in Damascus. *Nucl. Instrum. Methods Phys. Res. Sect. B* **2020**, *462*, 75–81. [[CrossRef](#)]
52. Li, J.; Chen, B.; Campa, A.M.; Alastuey, A.; Querol, X.; Rosa, J.D. 2005–2014 trends of PM₁₀ source contributions in an industrialized area of southern Spain. *Environ. Pollut.* **2018**, *236*, 570–579. [[CrossRef](#)] [[PubMed](#)]
53. Bencharif-Madani, F.; Ali-Khodja, H.; Kemmouche, A.; Terrouche, A.; Lokorai, K.; Naidja, L.; Bouziane, M. Mass concentrations, seasonal variations, chemical compositions and element sources of PM₁₀ at an urban site in Constantine, northeast Algeria. *J. Geochem. Explor.* **2019**, *206*, 106356. [[CrossRef](#)]
54. Jaafari, J.; Naddafi, K.; Yunesian, M.; Nabizadeh, R.; Hassanvand, M.S.; Ghozikali, M.G.; Shamsollahi, H.R.; Nazmara, S.; Yaghmaeian, K. Characterization, risk assessment and potential source identification of PM₁₀ in Tehran. *Microchem. J.* **2020**, *154*, 104533. [[CrossRef](#)]
55. Millán-Martínez, M.; Sánchez-Rodas, D.; Campa, A.M.; Rosa, J.D. Contribution of anthropogenic and natural sources in PM₁₀ during North African dust events in Southern Europe. *Environ. Pollut.* **2021**, *290*, 118065. [[CrossRef](#)] [[PubMed](#)]

Disclaimer/Publisher's Note: The statements, opinions and data contained in all publications are solely those of the individual author(s) and contributor(s) and not of MDPI and/or the editor(s). MDPI and/or the editor(s) disclaim responsibility for any injury to people or property resulting from any ideas, methods, instructions or products referred to in the content.